Bテトラマーに陽性であり，かつそれらの多くがsurv 2Bペプチド特異的に認識され，標的細胞を破壊することが示された。このようにあざやかなCTLのモニタリングが他の症例でも観察され，図4には進行膵癌の症例であるがvaccination後，ほぼ3年間以上もCA 19-9が正常値を保ち，テトラマー，ELISPOTともに明らかに検出され，これらCTLのソーテイングでもsurv 2Bペプチド特異的標的細胞障害も示された。これらの事実はsurv 2B + IFA + IFNαのプロトコールが癌患者でこのペプチド特異的CTLを誘導し，活性化し，それらが腫瘍局所で抗腫瘍効果を発揮していることを示唆するものといえる。表1に示した我々が同定した他のCTLエピトープも同様な期待がもたれる。それらが創薬化できるか否かについては地道な臨床試験をひとつずつ行い，長い時間は必要とするがピックアップしていくより他にない。持続的な基礎と臨床の腫瘍免疫研究者の努力が大切であり，互いに共通の目標に向かった高い志が必要なゆえんである。

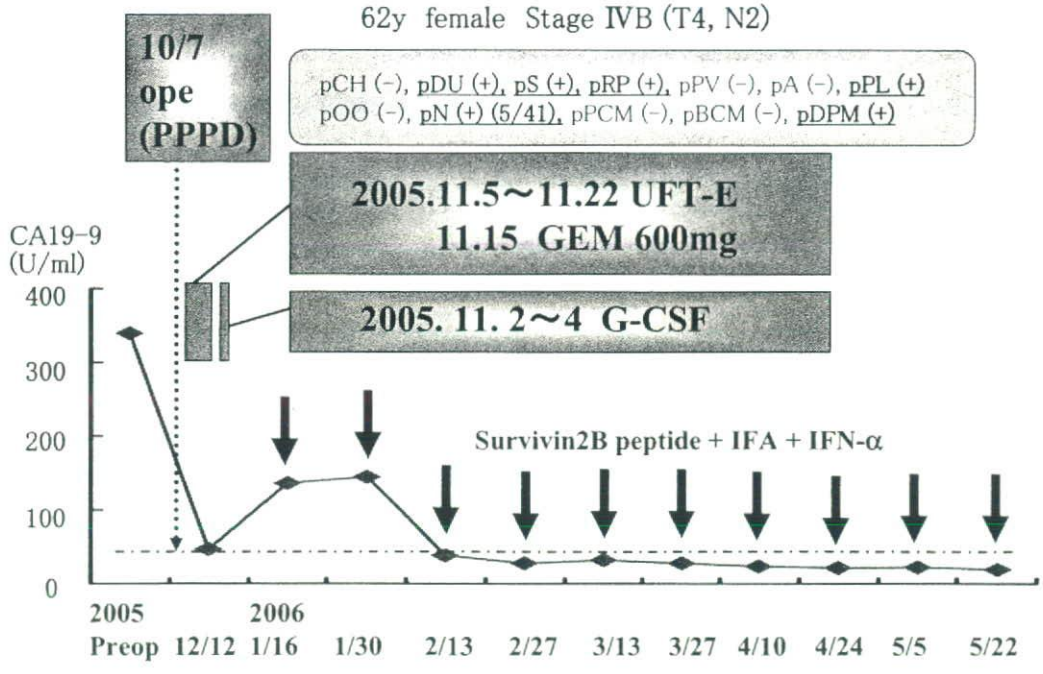


図4　症例6(膵癌)免疫応答と腫瘍マーカー推移
vaccination：Survivin-2B peptide + IFA + IFN-α

## 5　ヒト癌幹細胞（CSC）腫瘍抗原の同定と癌免疫治療への応用

上述のようにヒト腫瘍に発現する腫瘍抗原，さらにCTLが標的とするHLA提示CTLエピトープも多数同定され，臨床試験も世界中で行われているわけである。他方，免疫学的により優れた腫瘍抗原検索の研究も極めて大切である。すなわち，癌研究でトピックスになりつつある癌幹細胞と，これに発現する腫瘍抗原（cancer stem cell tumor antigens；CSC Ag）の同定である。我々はCSC Agの同定を，ほぼ20年前から研究着手していた。図5に示すようにラット正常胎児線維芽細胞WFB，あるいはBALB/Cマウス胎児線維芽細胞BALB/3T3に様々な活性型癌遺伝子をトランスフェクトし，様々なtumorigenic clonesを得た。例えばras癌遺伝子で得られたW31，Brashなどは$10^3$個で2Wで腫瘍形成を同系ラット，同系マウスにみせ，4Wでは1cm以上の径を示す極めて造腫瘍性の高いクローンであった。CSCのひとつの重要な特徴としてcancer initiating abilityが考えられているが，真にこの特徴を持つものであり，我々はWFB，BALB/3T3に発現なく，かつW31，Brashに高発現の細胞表面腫瘍抗原を単クローン抗体樹立により解析した。その結果，いくつかの抗原を得ることに成功し，ひとつはHSP（heat shock protein）70様の分子であり[16]，あるいはCD44であった[17]。2000年代に入り，とくに後者は様々なヒト腫瘍のCSCマーカーとなり得ることがわかり，我々の研究が基盤となった。し

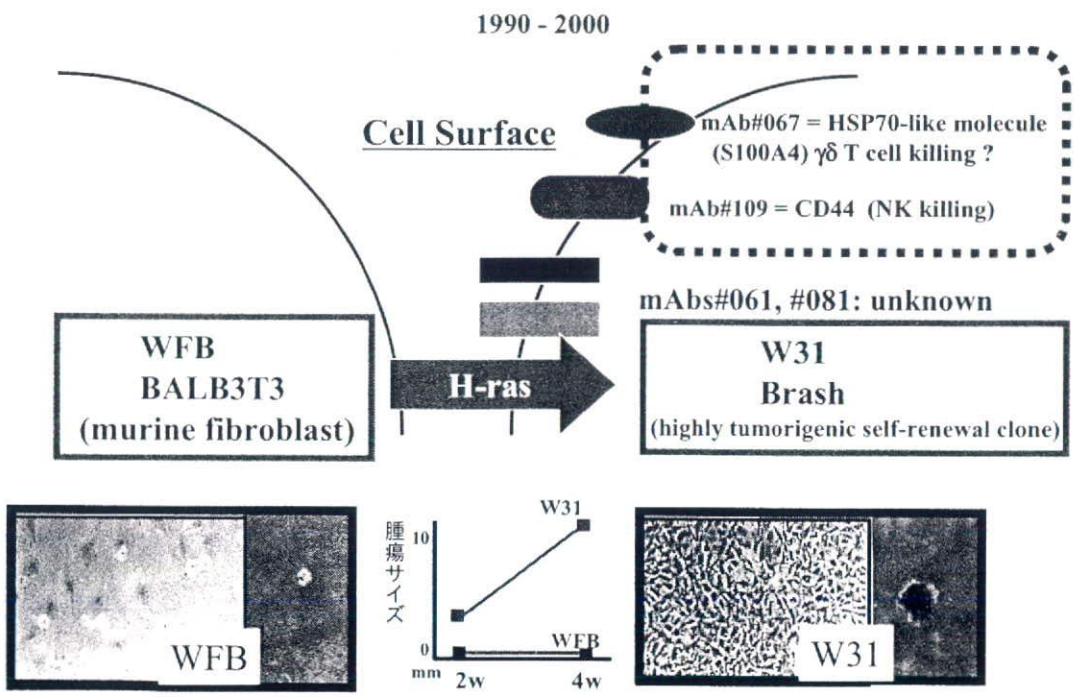


図5　Murine fibroblasts (WFB/BALB 3 T 3) の腫瘍化に伴う腫瘍抗原発現解析
－W 31 and Brash cells as cancer initiating cell counterparts－

かしCD 44は血管内皮等にも多量に発現し，腫瘍免疫の標的とすることは危険であり，他のCSC Agの探索を続けた。

数年前，CSCの多くがATP binding cassetteをもつABC transportersを発現していることが知られ，これを利用したCSC分離の可能性が示唆されていた。すなわちHoechst 33342等の色素染色を指標にするFACS上でのside population（SP）にCSCが集約される現象である。我々の解析結果に示すように腫瘍細胞によりこのSP technologyが有効であることが判った[1]。図6に示すようにLHK 2ヒト肺癌細胞株からSPとnon-SP（main population；MP）をソーティングし，NOD/SCIDマウスに移植した。その結果SP分画中の15個の細胞で明らかな腫瘍形成をみせ，一方，MP分画は150,000個の細胞が必要であった。すなわち，SP分画細胞は明らかなcancer initiating abilityを有していた。DNAマイクロアレイによりSP＞MPの腫瘍抗原を解析，その結果SP分画に発現するCSC Agを同定した。ひとつはcancer testis（CT）antigenの特徴を有するSMCP（sperm mitochondrial cystein-rich protein）であり，もうひとつはSOX-2であった。図7にはSOX-2のヒト乳癌の原発組織の免疫染色を示す。case 1のように多くの乳癌細胞がSOX-2を発現するも，むしろ多くのケースでcase 2のように一部の腫瘍細胞のみが発現していることが判った。我々はSOX-2のHLA-A 24提示CTLエピトープでもすでに決定しており，近日中にこの抗原ペプチドを用いた事CSC Agの世界ではじめての癌ワクチン臨床研究を開始する予定であり，成果が大いに期待される。

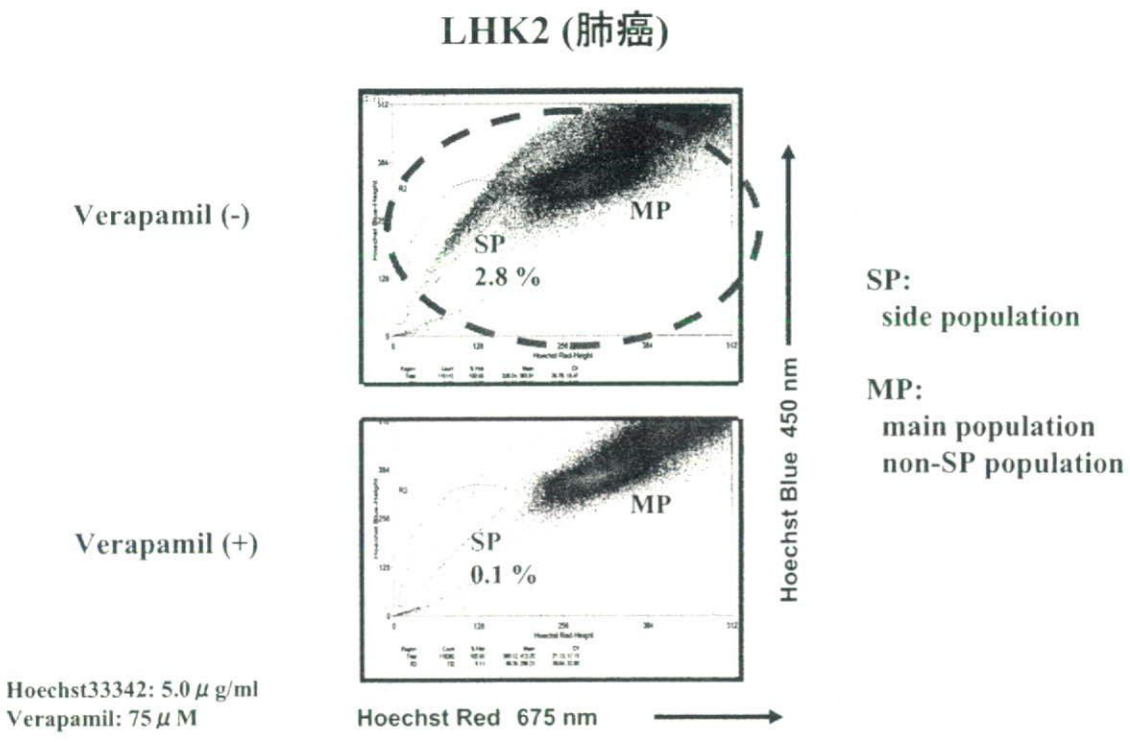


図6　Side Population (SP)

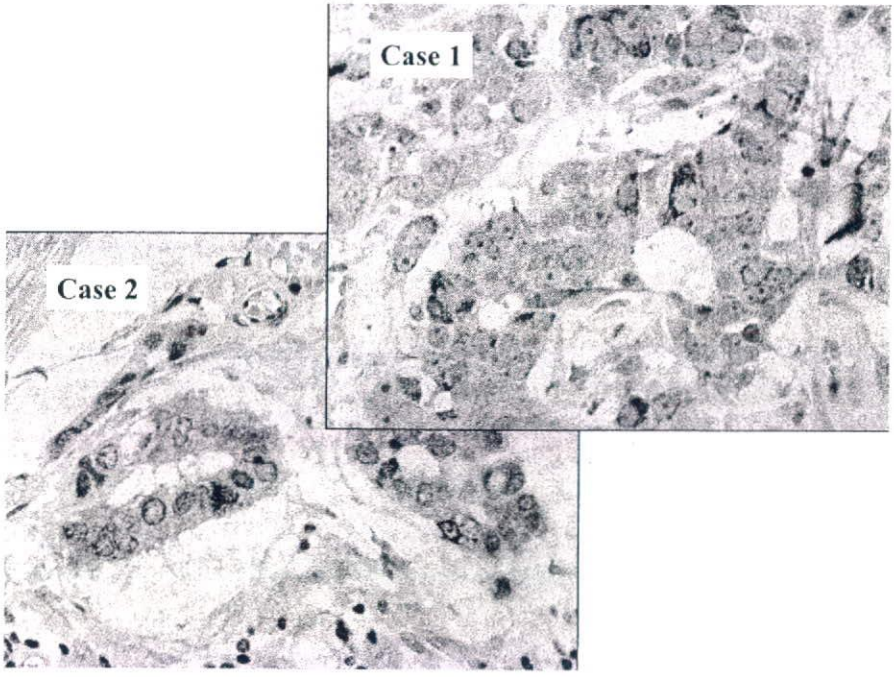


図7　乳癌 SOX-2 発現

## 6　癌ワクチン免疫原性の増強，制御

上に述べたような CTL が標的とし，かつ CTL 誘導，活性化する癌抗原蛋白，抗原ペプチドの持続的研究はヒト癌免疫研究の「いろは」の「い」であり，今もって最も重要である。他方，これらの抗原だけでは臨床的に有効な癌治療法のひとつとはなり得ないことも事実であろう。従ってこれらの抗原の免疫原性を増強する方法の開発も極めて重要である。古くよりいわゆるアジュバントと称し，様々な物質，製剤が存在するが，しかし，癌ワクチンにとり，その増強の機構がロジカルに判明し，CTL を誘導することが判っているのは実際のところない。これからの重要な研究テーマである理由でもある[1,18~21]。

我々は，このような背景のもと，癌抗原の免疫原性の増強に重要な分子の同定を進めてきた。その結果，熱ショック蛋白質（heat shock protein；HSP）のあるものがこのような活性を選択的にもつことが明らかにされつつある[1]。図 8 に示すように近年，抗原提示細胞である樹状細胞（DC）やマクロファージの活性化（自然免疫活性化）機構が解明された。すなわち TLR，non-TLR などが自然免疫活性化に重要な APC 細胞表面あるいは細胞内受容体として明らかにされたわけである[20]。感染症で外因性リガントとして細菌 LPS やウイルス核酸の様々な分子が働くことがわかっている。一方，内因性リガントのひとつの重要な分子として HSP も知られ，HSP 60 は TLR 2，HSP 70 は TLR 4 を受容体とする。HSP 90 は未だどのような受容体かは不明であ

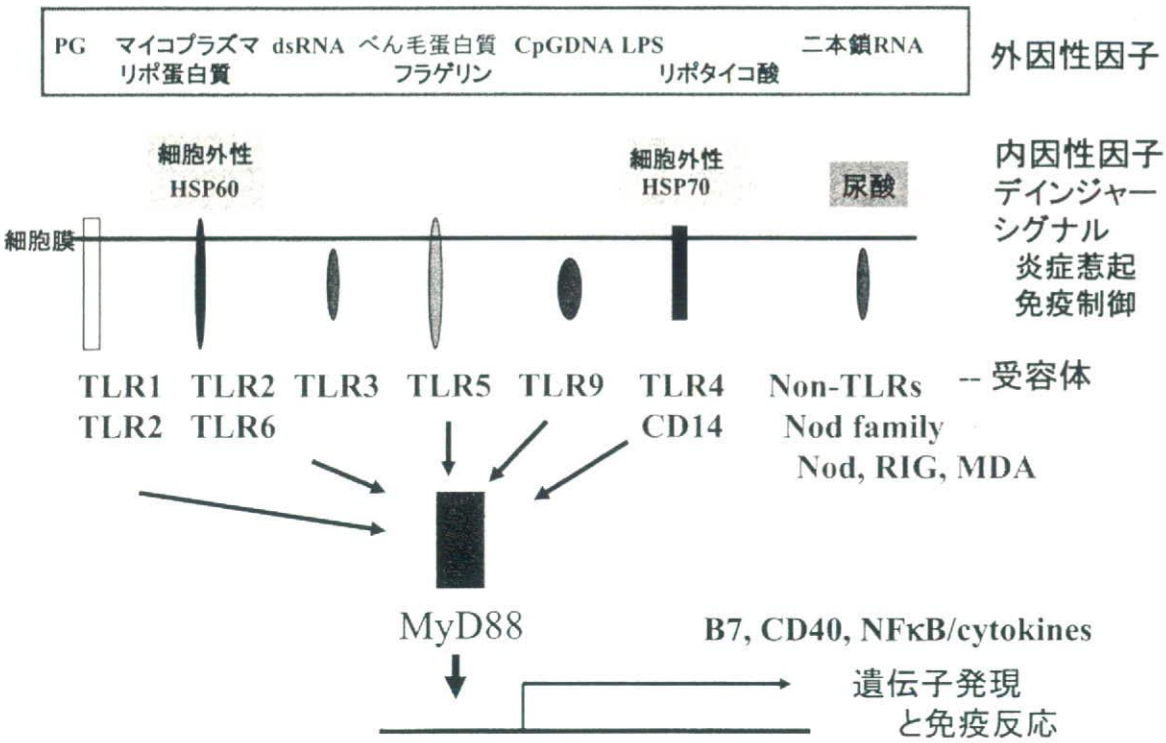


図 8　自然免疫活性化に関わる外因性因子，内因性因子と受容体

るが，DC に外から HSP 90 を加えると IFN $\alpha$ を効率よく産生する。

これら HSP が外因性リガントと決定的に異なる側面は HSP が分子シャペロンであり，抗原蛋白，抗原ペプチドを含む種々の分子と会合状態にあり，それら複合体の形で，DC に取り込まれることである。例えば HSP 90 と癌抗原ペプチド結合体を作り DC に取り込まれると，DC 内で抗原ペプチドの MHC クラス I ルートへの提示，すなわちクロス提示が大変有効になされることが，我々の研究より明らかにされた。CTL の誘導効率は現在最も強力なアジュバントとされる CFA に匹敵する[19]。*In vivo* の腫瘍拒絶モデルで，このことを実証した（図 9）。すなわち，HLA-A*2402 トランスジェニックマウスに発癌剤メチルコラントレンを投与し，形成された皮膚腫瘍から TG 3 細胞を株化し，さらに TG 3 にサバイビン 2 B 遺伝子を移入し，TG 3-surv 2 B を樹立した。この細胞をトランスジェニックマウスに移植し，HSP 90-surv 2 B ペプチド複合体を vaccination すると，ペプチド単独より明らかな腫瘍増強低下をみせた。HSP 90 はその結合体を初期エンドソームにある一定時間とどめることを我々は独自に観察している。例えば HSP 90 と CpGDNA の結合体も初期エンドソームに処理後 2 時間の長きにわたりとどまる。その結果，CpGDNA 単独では IFN $\alpha$ 誘導を示さない cDC（conventional DC）も HSP 90-CpGDNA では示すようになった。

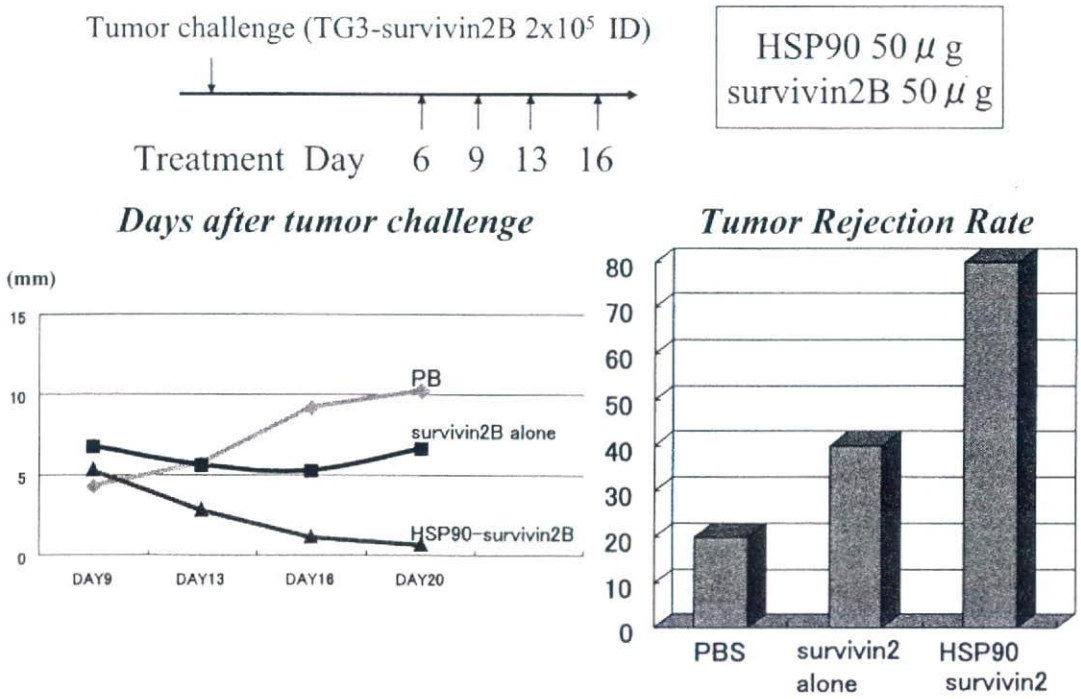


図9　細胞外性 HSP 90-survivin 2 B がんペプチド複合体による *in vivo* 免疫増強

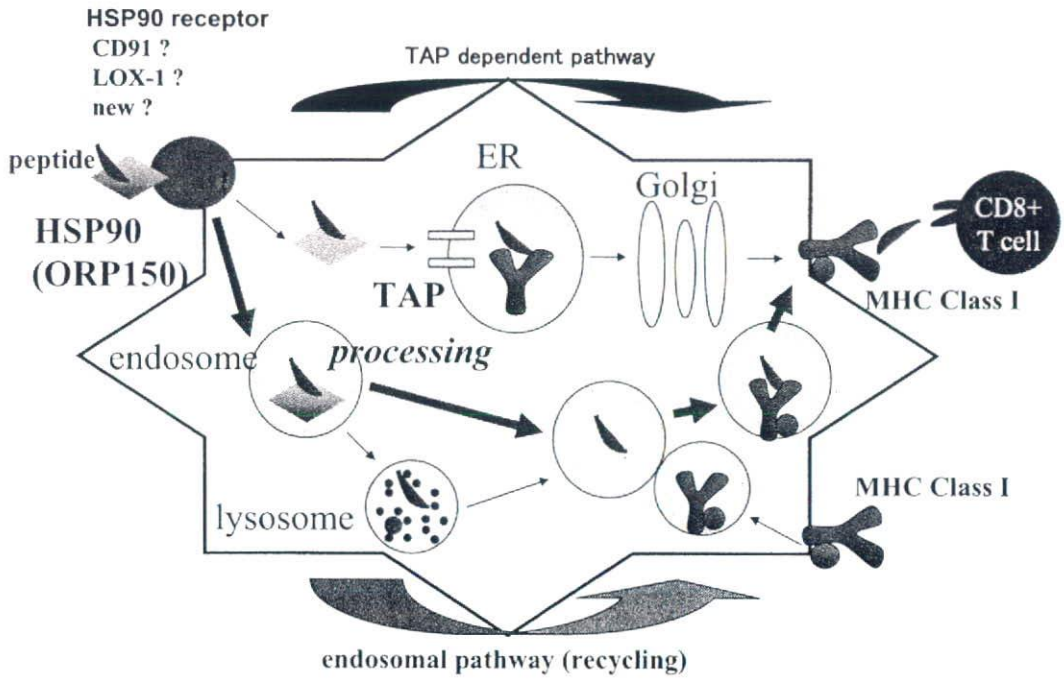


図10　細胞外性の HSP 90 結合抗原ペプチドはエンドゾーム経由で HLA クラス I に高効率で交叉提示される

以上のようにHSP 90はDCを①サイトカイン産生活性に導くばかりでなく，②CTLエピトープのクロス提示，相方を担う免疫増強性因子であることが示唆された（図10）。

## 7　免疫抑制の解除

腫瘍に免疫学的なエスケープ機序が存在することが明らかであり，多くの事実が今日まで示されている。様々な側面のうち，最も代表的なものはMHC class I分子の発現低下である。我々はこの課題を解析するため，数年前に病理パラフィン切片上でも検出可能な抗HLA-クラスI単クローン抗体（EMR 8-5）を樹立した（すでに市販化）。その結果，驚いたことに乳癌および前立腺癌では80%以上の症例でHLA-クラスIが大きく発現低下していることが判明した。その機序を解析したところ，多くの症例でβ2ミクログロブリン（B2M）遺伝子領域のエピジェネティックな制御による発現低下であることが判明した。特にヒストン脱アセチル化（HDAC）によるものであることがわかり，HDACのうち，HDACIあるいはHDAC 3酵素の発現上昇によるものであることが示唆された。こうなるとHDAC阻害剤によるB2M-HLAクラスI分子の発現回復の可能性が出てくるが，図11に示すようにその可能性が確認された。すなわちHDAC阻害剤バルプロ酸（デパケン）処理によりヒトMCF 7乳癌にB2M，HLAクラスI重鎖の発現が明らかに増しており，また細胞表面発現の回復もみられた。このことはHDAC阻害剤によ

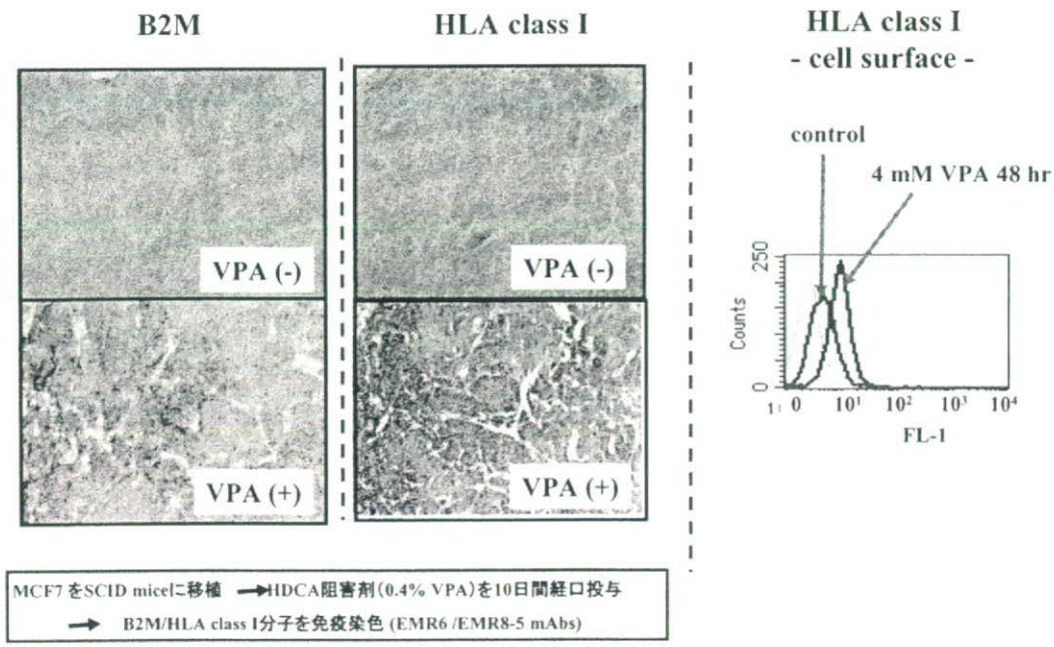


図11　HDAC阻害剤（VPA）投与によるB2M/HLA class I分子 *in vivo* 発現回復

る有効な免疫治療の底上げがなされることを意味しており，今後の臨床試験等を含めた取り組みが期待されている[1,22~24]。

## 8　おわりに

以上のようにヒト腫瘍抗原の同定，その臨床試験，癌抗原免疫原性の増強，免疫エスケープの解除等について我々の研究成果を中心にして述べた。癌の免疫による制御をどの程度ヒトでできるのかはまだまだわからない。しかし，一歩一歩確実に前進しているのは事実である。臨床試験と基礎研究を並行し，互いにクロスオーバーさせることにより，癌の治療のひとつの方法として免疫があることが，必ずや実現されると思われる。

## 文　　献


1）N. Sato *et al.*, *Pathol. Int.*, in press.
2）河野修己，特異抗原で開発加速 新型抗がん剤の一翼，がん治療ワクチン，日程バイオテク，ビジネスレビュー，10-6，3-7（2008）
3）T. Tsukahara *et al.*, *Cancer Res.*, **64**, 5442-5448（2004）
4）T. Tsukahara *et al.*, *Cancer Sci.*, **99**, 368-375（2008）
5）K. Suzuk *et al.*, *J. Immunol.*, **163**, 2783-2791（1999）
6）H. Sahara *et al.*, *J. Immunother*, **25**, 235-242（2002）
7）Y. Hirohashi *et al.*, *Clin. Cancer Res.*, **8**, 1731-1739（2002）
8）S. Idenoue *et al.*, *Clin. Cancer Res.*, **11**, 1474-1482（2005）
9）Y. Sato *et al.*, *J. Immunol.*, **169**, 1611-1618（2002）
10）K. Ida *et al.*, *J. Immunol.*, **173**, 1436-1443（2004）
11）E. Sato *et al.*, *Clin. Cancer Res.*, **14**, 6916-6923（2008）
12）T. Tsuruma *et al.*, *J. Transl. Med.*, **2**, 19-29（2004）
13）T. Tsuruma *et al.*, *J. Transl. Med.*, **6**, 24-35（2008）
14）S. Kawaguchi *et al.*, *J. Transl. Med.*, **3**, 1（2005）
15）T. Tsuruma *et al.*, *Expert Opin. Biol. Ther.*, **5**, 799-807（2005）
16）A. Konno *et al.*, *Cancer Res.*, **49**, 6578-6582（1989）
17）K. Kanki *et al.*, *Microbiol. Immunol.*, **44**, 1051-1061（2000）
18）S. Takashima *et al.*, *J. Immunol.*, **157**, 3391-3395（1996）
19）T. Kurotaki *et al.*, *J. Immunol.*, **179**, 1803-1813（2007）
20）Y. Tamura *et al.*, "Extracellular heat shock proteins in immune response: A guide

for cross-presentation." Heat Shock Proteins in Biology and Medicine, 119-130 (2006)
21) G. Ueda *et al.*, *Cancer Sci.*, **95**, 248-253 (2004)
22. T. Tukahara *et al.*, *Cancer Sci.*, **97**, 1374-1380 (2006)
23) H. Kitamura *et al.*, *J. Urology*, in press.
24. T. Kanaseki *et al.*, *J. Immunol.*, **170**, 4980-4985 (2003)

THE JOURNAL OF BIOLOGICAL CHEMISTRY VOL. 282, NO. 37, pp. 26956–26962, September 14, 2007


# Biological Heterogeneity of the Peptide-binding Motif of the 70-kDa Heat Shock Protein by Surface Plasmon Resonance Analysis*

Received for publication, April 25, 2007, and in revised form, June 29, 2007 Published, JBC Papers in Press, July 11, 2007, DOI 10.1074/jbc.M703436200

**Hideki Maeda**[‡§], **Hiroeki Sahara**[¶1], **Yoko Mori**[¶], **Toshihiko Torigo**[§], **Kenjiro Kamiguchi**[§], **Yutaka Tamura**[‖], **Yasuaki Tamura**[§], **Kouichi Hirata**[‡], **and Noriyuki Sato**[§]

*From the Departments of* [‡]*Surgery and* [§]*Pathology and the* [¶]*Marine Biomedical Institute, Sapporo Medical University School of Medicine, South 1 West 17, Chuo-ku, Sapporo 060-8556, Japan and the* [‖]*Department of Bioinformatics Graduate School of Medicine, Chiba University, 1-8-1, Inohana, Chiba 260-8670, Japan*

**70-kDa heat shock protein family is a molecular chaperone that binds to a variety of client proteins and peptides in the cytoplasm. Several studies have revealed binding motifs between 70-kDa heat shock protein family and cytoplasmic proteins by conventional techniques such as phage display library screening. However, little is known about the binding motif based on kinetic parameters determined by surface plasmon resonance analysis. We investigated the major inducible cytosolic 70-kDa heat shock protein (Hsp70)-binding motif with the human leukocyte antigen B*2702-derived peptide Bw4 (RENLRIALRY) by using a Biacore system based on surface plasmon resonance analysis. The $K_D$ value of Hsp70-Bw4 interaction was $1.8 \times 10^{-6}$ M. Analyses with truncated Bw4 variant peptides showed the binding motif of Hsp70 to be seven residues, LRIALRY. To further study the characteristics of this motif, 126 peptides derived from Bw4, each with single amino acid substitution, were synthesized and analyzed for Hsp70 binding affinity. Interestingly, the Hsp70 binding affinity was abrogated when the residues were substituted for by acidic (Asp and Glu) ones at any position. In contrast, if the substitute residue was aromatic (Trp, Tyr, and Phe) or an Arg residue at any position, Hsp70 binding affinity was maintained. Thus, this study presents a new binding motif between Hsp70 and peptides derived from the natural protein human leukocyte antigen B*2702 and may also elucidate some characteristics of the Hsp70 binding characteristic, enhancing our understanding of Hsp70-binding determinants that may influence diverse cellular and physiological processes.**

Molecular chaperones of the 70-kDa heat shock protein family perform numerous functions in the quality control of cells that mediate protein folding, translocation, assembly/disassembly, and repair of unfolded proteins damaged by environmental stress (1). Chaperone activity of this protein family is necessary to recognize binding sites of a target native protein, referred to as the binding motif. It has been reported that the endoplasmic reticulum 70-kDa heat shock protein Bip (Grp78) binds to a peptide containing at least seven residues with maximal affinity in the presence of ATPase activity (2, 3). It was also suggested that peptide-binding sites of Bip show a preference for sequences rich in aliphatic residues. Subsequently, from a study employing a phage display library, the binding motif for Bip was revealed to be a heptapeptide with high contents of aromatic and hydrophobic residues (4).

On the other hand, the bacterial cytoplasmic 70-kDa heat shock protein homolog DnaK has a substrate-binding region in the C terminus, and repeated binding/release to substrates is dependent on the ATPase cycle at an ATPase domain of the N terminus (5, 6). Zhu *et al.* (7) reported a crystal structure of the C-terminal substrate-binding domain of DnaK, which was located in a hydrophobic substrate-binding cleft with a central pocket placed between a $\beta$ sheet and two $\alpha$ helices. The consensus motif recognized by DnaK consisted of peptides comprising a hydrophobic core of 4–5 residues flanked by basic residues (8). Moreover, in virus-infected cells, it is well known that a 60-kDa heat shock protein (Hsp60)[2] and a 90-kDa heat shock protein (Hsp90) bind to hepatitis B virus-derived proteins such as polymerase and transcriptase (9, 10). Recently, it was reported that the host major inducible cytosolic 70-kDa heat shock protein (Hsp70)-binding motif interacted with a heptapeptide from a nucleoprotein of measles virus (11) and stimulated transcriptional activities of this virus (12, 13). Thus, the 70-kDa heat shock protein family is capable of recognizing and binding not only to the structural region of a protein but also to a specific localized peptide motif.

Although 70-kDa heat shock protein family-binding motifs derived from observations of interactions with its many substrate proteins have been proposed, little is known about the binding motif based on kinetic parameters determined by surface plasmon resonance (SPR) analysis. Because target molecules basically bind to 70-kDa heat shock protein in low affinity interactions, it might be difficult to measure binding interaction by conventional methods such as competitive immunoprecipitation.

* This work was supported by Grants-in-aid for Scientific Research 16209013 and 15659097 from the Ministry of Education, Culture and Science of Japan (to N. S.). The costs of publication of this article were defrayed in part by the payment of page charges. This article must therefore be hereby marked "*advertisement*" in accordance with 18 U.S.C. Section 1734 solely to indicate this fact.

[1] To whom correspondence should be addressed: South 1 West 17, Chuo-ku, Sapporo 060-8556, Japan. Tel.: 81-11-611-2111; Fax: 81-11-612-5861; E-mail: hsahara@sapmed.ac.jp.

[2] The abbreviations used are: Hsp, heat shock protein; Hsc, heat shock cognate protein; SPR, surface plasmon resonance; HLA, human leukocyte antigen; RU, resonance unit.

The use of SPR technology, on which bimolecular interaction analysis (Biacore) is based, provides us with the most expedient approach for measurement of low affinity protein interactions in real time. With the Biacore system, one interaction partner is conjugated on the surface of a sensor chip (ligand), and other binding partners flow over the surface (analyte), facilitating analysis of binding differences between multiple analytes and a single ligand. In this study, we investigated the interaction of Hsp70 with the HLA-B*2702-derived peptide Bw4 (RENLRIALRY, HLA-B*2702 amino acids 75–84) and its various truncated and substituted peptides using a Biacore system. Nössner *et al.* (14) reported that Bw4 can bind to Hsp70 and 70-kDa heat shock cognate protein (Hsc70) and elicit a suppressive effect on T cell function. Because the Hsp70-binding motif basically is a heptapeptide, the aim of this study was to find a new Hsp70-binding motif and its biologic characteristics, if present, using the Biacore system.

Consequently, we demonstrated that Hsp70 bound to Bw4 with $K_D = 1.8 \times 10^{-6}$ M. Using truncated and Ala-substituted variants of Bw4, the Hsp70-binding motif of Bw4 was newly found to be heptapeptide LRIALRY. Moreover, we found that if residues in this motif were substituted for by an aromatic (Trp, Tyr, and Phe) or Arg residue at any position, Hsp70 binding affinity was maintained, whereas with acidic residue substitutions, binding affinity to Hsp70 was markedly decreased. The present study suggests a new binding motif between human Hsp70 and peptides derived from natural protein HLA-B*2702 and also discloses characteristics of the Hsp70-binding motif structure. Our findings may contribute to enhanced understanding of 70-kDa heat shock protein family binding determinants that may influence diverse cellular and physiological processes.

## EXPERIMENTAL PROCEDURES

*70-kDa Heat Shock Proteins and Synthetic Peptides*—Recombinant human Hsp70 protein (NSP-555), the endoplasmic reticulum 70-kDa heat shock protein Bip (Grp78) (SPP-765), and *Escherichia coli* DnaK protein (SPP-630) were purchased from StressGen (Victoria, Canada). All of the peptides were synthesized by Sigma-Aldrich. The peptides were dissolved with 5% $Me_2SO$ (Merck) in phosphate-buffered saline at the indicated concentrations in each experiment.

*Surface Plasmon Resonance Analysis using the Biacore System*—SPR experiments were performed with a Biacore 3000 system (Biacore, Inc., Uppsala Sweden). With this system, molecules of interest (ligands) are immobilized on a sensor surface, and binding partners (analytes) can then be passed over it in a mobile aqueous phase. Their interaction on the sensor surface can subsequently be monitored in real time without the use of labels. To investigate Hsp70-, Bip-, and DnaK-peptide interactions, we employed Hsp70, Bip, and DnaK proteins as ligands that were immobilized on the sensor surface, and Bw4 (RENLRIALRY, HLA-B*2702 amino acids 75–84) and Bw6 (RESLRNLRGY, HLA-B*0701 amino acids 75–84) peptides as the analytes. It is known that Bw4, but not Bw6, can bind to Hsp70/Hsc70 and elicit a suppressive effect on T cells (14). In addition, truncated and amino acid-substituted peptides of Bw4 also were used as analytes.

Hsp70, Bip, and DnaK were immobilized by amine coupling methods, according to the instruction manual for the Biacore 3000, which utilizes a primary amino group of proteins for covalent attachment to the matrix. Briefly, a dextran layer on a sensor chip that is covalently attached to a carboxymethylated dextran gold surface (CM5 sensor chip; Biacore, Inc.) was activated by injection of a mixture of *N*-hydroxysuccinmide and carbodiimide, creating a reactive ester on the surface for 10 min. Subsequently, 100 μl of 20 μg/ml ligand in 10 mM sodium acetate (pH 5.5) was injected for 10 min and loaded with 1 M ethanolamine for 10 min to block binding to remaining nonreacted ester groups. Finally, the chip surface was washed with running buffer (5% $Me_2SO$, 2.5 mM magnesium acetate, 2.5 mM ATP (disodium salt; Sigma) in phosphate-buffered saline) to remove any loosely bound ligands. The amounts of immobilized Hsp70, Bip, and DnaK as ligands were 19,000, 14,347, and 7,843 resonance units (RU), respectively, corresponding to sensor surface areas of ~19, 14.3, and 7.8 ng/mm$^2$, respectively.

To estimate these ligand-peptide interactions, the affinity of the interaction, *i.e.* the equilibrium dissociation constant ($K_D$), was determined from the level of binding at equilibrium as a function of the sample concentrations by BIAevalution version 4.1 software (Biacore, Inc.). All of the peptides were dissolved with running buffer including 5% $Me_2SO$, and binding experiments were performed at 25 °C in running buffer with a flow rate of 20 μl/min. To reduce errors in reference subtraction, solvent effects were compensated for by a $Me_2SO$ calibration procedure according to the BIAcore manufacturer's instructions. All of the peptide responses were corrected for $Me_2SO$ bulk differences via the $Me_2SO$ calibration curves that were obtained by the $Me_2SO$ calibration procedures performed at the beginning and end of each experiment.

## RESULTS

The Biacore assay based on SPR was used to monitor the Hsp70-, Bip-, and DnaK-peptide interactions. SPR detects molecular interactions because there is a corresponding change in the refractive index if binding occurs as a peptide passes over a prepared sensor surface. The responses on the sensorgram are designated RU. We initially attempted to estimate the binding affinity between Hsp70 and the Bw4 or Bw6 peptide. Each peptide was injected at a concentration of 50 μM for 2 min at a flow rate of 20 μl/min to detect the association phase and loaded with running buffer alone on the sensor chip for 2 min at a flow rate of 20 μl/min to detect the dissociation phase. As shown in Fig. 1*A*, the immobilized Hsp70 on the sensor chip bound to Bw4 peptide, whereas Bw6 exhibited low binding compared with the Hsp70-Bw4 interaction. Bw4 binding to Hsp70 tended to be extremely fast, reaching equilibrium immediately after Bw4 peptide injection, and the complex dissociated just as quickly when the flow was switched to a running buffer, with RU returning to the basal level. Therefore, it was difficult to calculate the kinetic parameters ($K_a$ and $K_d$) directly. The affinity of interaction was determined from the level of binding at equilibrium as a function of the sample concentration, which is referred to as the equilibrium dissociation constant ($K_D$).

We attempted to estimate the binding affinity in the Hsp70-Bw4 interaction. Bw4 peptide in concentrations ranging from

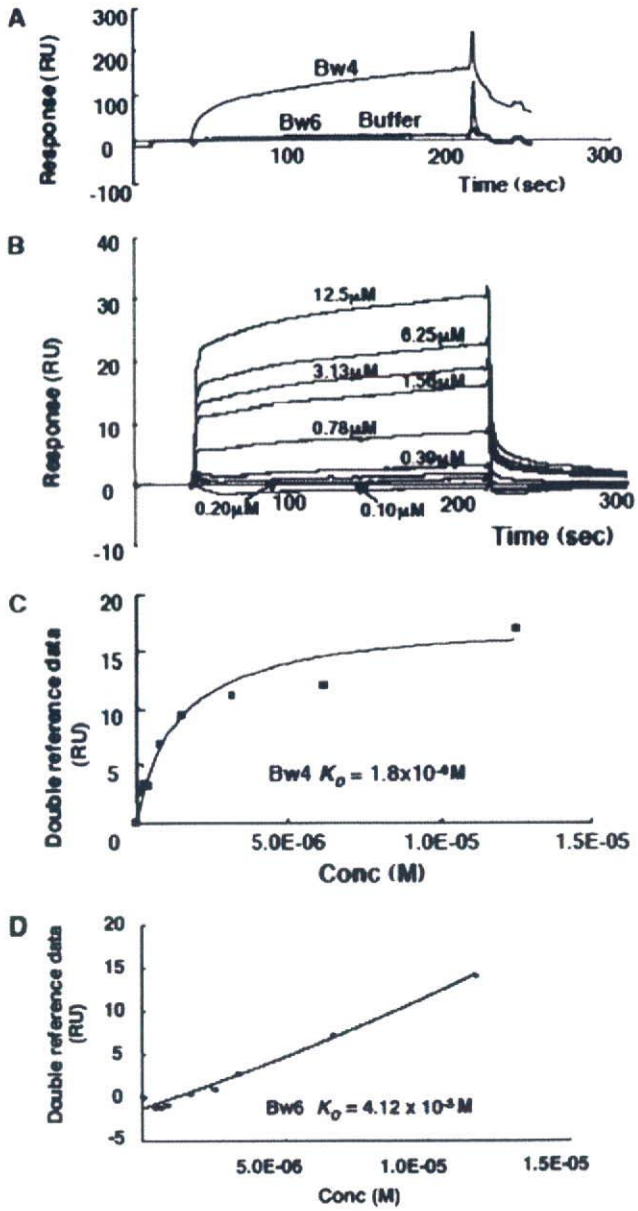


FIGURE 1. **The binding of human Hsp70 to peptides Bw4 and Bw6.** *A*, Biacore 3000 sensorgrams illustrating binding of synthetic peptides Bw4 and Bw6 to immobilized Hsp70. Each 50 μM peptide solution was passed over sensor chips on which 19,000 RU of Hsp70 was immobilized. Retention of a peptide on a sensor chip was indicated by a change in RU over the course of the 200-s injection interval. *B*, overlay plot of sensorgrams of interaction of Bw4 peptide with Hsp70. Bw4 peptides in concentrations (*Conc*) of 0.1, 0.2, 0.39, 0.78, 1.56, 3.13, 6.25, and 12.5 μM were injected over the Hsp70 sensor chip, and the magnitude of Bw4 binding to immobilized Hsp70 was analyzed. *C* and *D*, a kinetic plot and binding isotherm for binding of Bw4 or Bw6 to the Hsp70 sensor chip in peptide concentrations ranging from 0.1 to 12.5 μM. Binding affinity was determined from the level of binding at equilibrium as a function of the sample concentration using BIAevaluation version 4.1 software and referred to as the equilibrium dissociation constant ($K_D$).

0.1 to 12.5 μM was injected over an Hsp70 sensor chip for 2 min at a flow rate of 20 μl/min and loaded with running buffer alone for 2 min at the same flow rate. Association and dissociation phases of the Hsp70-Bw4 interaction at each concentration were shown to occur in a dose-dependent manner (Fig. 1*B*). Subsequently, kinetic analysis based on these data were performed, and the equilibrium dissociation constant ($K_D$) was determined using BIAevalution (version 4.1) software. As shown in Fig. 1*C*, a specific binding response between Hsp70 and Bw4 was observed, and the estimated $K_D$ for binding was $1.8 \times 10^{-6}$ M. On the other hand, as shown in Fig. 1*D*, the estimated $K_D$ for binding between Hsp70 and Bw6 in the same manner was found to be $4.12 \times 10^{-3}$ M, indicating that this binding affinity was ~440-fold lower than the Hsp70-Bw4 interaction.

We also tried to determine whether peptide binding affinity to isotypes of the 70-kDa heat shock protein family such as mammalian endoplasmic reticulum-resident Bip and prokaryotic DnaK molecules was different from Hsp70-Bw4 or -Bw6 interactions. As shown in Fig. 2 (*A* and *B*), it was somewhat surprising that the estimated $K_D$ values for binding of Bw4 to Bip and DnaK were $3.72 \times 10^{-3}$ M and $1.85 \times 10^{-4}$ M, respectively, indicating that Bip and DnaK had low binding affinity as compared with Hsp70. In terms of interactions with Bw6, the estimated $K_D$ values for binding to Bip and DnaK were $9.0 \times 10^{-4}$ M and $4.83 \times 10^{-3}$ M, respectively (Fig. 2, *C* and *D*).

To investigate characteristics of the binding motif of Hsp70-Bw4 interaction, truncated Bw4 variant peptides were employed. The truncated Bw4 peptides presented in Table 1 were injected over an Hsp70 sensor chip in a similar manner. Truncated 9-, 8-, and 7-mer Bw4 peptides from which N-terminal Arg, Arg-Glu, and Arg-Glu-Asn residues were deleted, respectively, interacted with Hsp70 with high affinity ($K_D < 5 \times 10^{-6}$ M), as did the wild type, but 6-mer (or fewer) peptides could not bind ($K_D > 1 \times 10^{-3}$ M) to Hsp70 (Table 1). In contrast, truncated Bw4 peptides with deletion of only a C-terminal Tyr did not show interaction with Hsp70 ($K_D > 1 \times 10^{-3}$ M), indicating that a C-terminal Tyr residue was critical for binding to Hsp70 and that the end of the binding motif of the C terminus seemed to be Tyr-84 of HLA-B*2702. Therefore, the Hsp70-binding motif interacting with Bw4 was 7-mer amino acid residues, LRIALRY, designated N3-Bw4. We also determined the $K_D$ value of this peptide. As shown in Fig. 3, the $K_D$ for binding between Hsp70 and N3-Bw4 peptide was estimated to be $2.6 \times 10^{-6}$ M.

Next, key amino acid residues in the motif of Bw4 binding to Hsp70 were studied using synthetic alanine-substituted peptides. Nine of these peptides were loaded over an Hsp70 sensor chip as above. We found that R1A, E2A, and N3A peptides that substituted for alanine at Arg-1, Glu-2, and Asn-3, respectively, maintained high affinities ($K_D < 5 \times 10^{-6}$ M), like the wild type (Table 2), indicating that three N-terminal residues without binding motifs could not influence Hsp70 binding affinity. However, other alanine substitutions at L4A, R5A, I6A, L8A, R9A, and Y10A resulted in loss of binding ($K_D > 1 \times 10^{-3}$ M) to Hsp70 (Table 2). Thus, it was demonstrated that each amino acid residue in the binding motif LRIALRY was critical for binding of Hsp70-Bw4 peptides.

Subsequently, characteristics of the Hsp70-peptide-binding motif were investigated using a peptide array. An array of single amino acid-substituted peptides, which consisted of 126 peptides, of Bw4 wild peptide (10-mer peptide), was synthesized. For example, in the case of substituted peptides at position 8 of the N terminus, a Leu residue was substituted for by 18 amino acid residues: L8W, -Y, -F, -R, -K, -H, -M, -I, -V, -T, -A, -Q, -G, -P, -N, -S, -D, and -E. Cys substitutions were not performed in

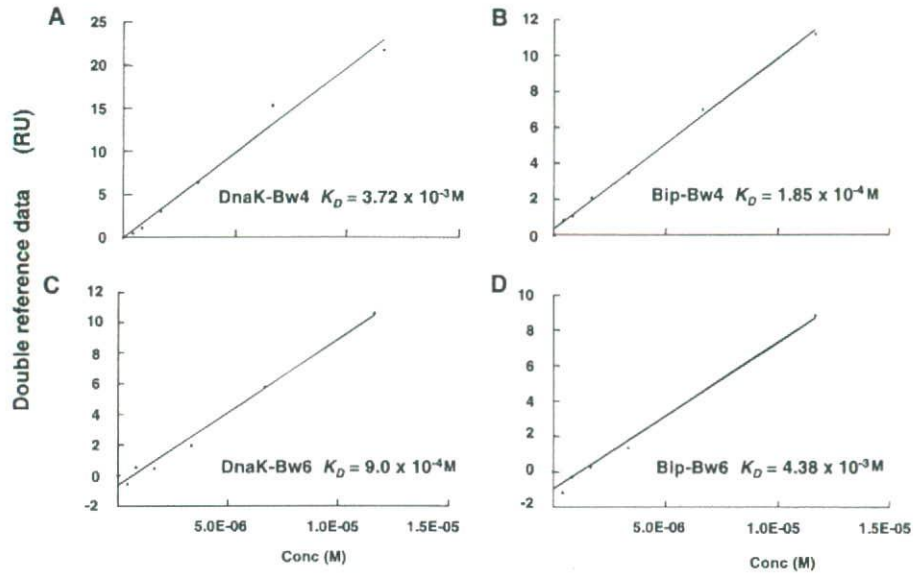


FIGURE 2. **A kinetic plot and binding isotherm for binding of Bw4 to Bip (*A*) and DnaK (*B*) sensor chips and of Bw6 to Bip (*C*) and DnaK (*D*) sensor chips in concentrations ranging from 0.1 to 12.5 $\mu$M.** The $K_D$ value was determined using BIAevaluation version 4.1. *Conc*, concentration.

**TABLE 1**
Binding assay of truncated Bw4 peptides

| Name | Sequence of truncated peptide | Binding affinity ($K_D$) |
|---|---|---|
| | | M |
| Bw4 | RENLRIALRY | $1.8 \times 10^{-6}$ |
| N1-Bw4 | ENLRIALRY | $1.9 \times 10^{-6}$ |
| N2-Bw4 | NLRIALRY | $1.3 \times 10^{-6}$ |
| N3-Bw4 | LRIALRY | $2.6 \times 10^{-6}$ |
| N4-Bw4 | RIALRY | $>10^{-3}$ |
| N5-Bw4 | IALRY | $>10^{-3}$ |
| C1-Bw4 | RENLRIALR | $>10^{-3}$ |
| C2-Bw4 | RENLRIAL | $>10^{-3}$ |
| C3-Bw4 | RENLRIA | $>10^{-3}$ |
| C4-Bw4 | RENLRI | $>10^{-3}$ |
| C5-Bw4 | RENLR | $>10^{-3}$ |

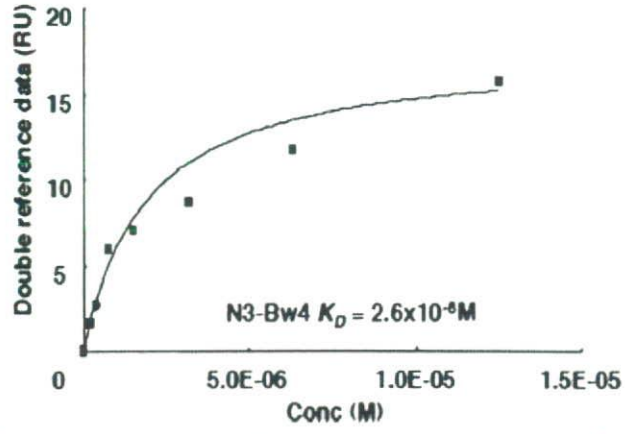


FIGURE 3. **A kinetic plot and binding isotherm for binding of the 7-mer peptide variant derived from Bw4 to the Hsp70 sensor chip in concentrations ranging from 0.1 to 12.5 $\mu$M.** The $K_D$ value was determined using BIAevaluation version 4.1. *Conc*, concentration.

this study to avoid multimerization among substituted peptides by S-S binding. All of the peptides were loaded over an Hsp70 sensor chip in a similar manner. As shown in Fig. 4, single amino acid-substituted peptides in white squares represent the high affinity with Hsp70 ($K_D < 5 \times 10^{-6}$ M), whereas peptides in *blue squares* represent decreased binding affinity ($K_D > 1 \times 10^{-3}$ M). Peptides, except for R5Y, with aromatic residues (Trp, Tyr, and Phe) and Arg substitution showed high affinity with Hsp70, like the wild type, at any position, whereas acidic residue (Asp and Glu)-substituted peptides lost their binding affinity ($K_D > 1 \times 10^{-3}$ M).

The estimated $K_D$ values for binding between the Hsp70 and five peptides with aromatic Ile or Arg substituted at position 8 are shown in Fig. 5. These peptides in concentrations ranging from 0.1 to 12.5 $\mu$M, were injected over an Hsp70 sensor chip for 2 min at a flow rate of 20 $\mu$l/min and loaded with running buffer alone for 2 min at the same flow rate. Specific binding affinity interaction between Hsp70 and these peptides was observed, and the estimated $K_D$ values for binding of L8Y, -W, -F, -R, and -I were 6.7, 1.1, 1.4, 1.4, and $1.8 \times 10^{-6}$ M, respectively, indicating binding affinity mostly similar to the wild type. Thus, as shown in Fig. 6, it appears that aromatic and Arg residues are favored residues for interaction with Hsp70, whereas acidic residues are not favored.

## DISCUSSION

The present study demonstrated, by SPR analysis, a new HLA-derived heptapeptide-binding motif, LRIALRY, interacting with human Hsp70. Nössner *et al.* (14) reported that the Bw4 peptide bound to Hsp70/Hsc70 and elicited a suppressive effect on T cell function. Bw4, consisting of a 10-mer peptide, is derived from the most polymorphic region in the $\alpha$1 domain of HLA-B*2702, where it is important for self and nonself recognition by T cell receptors. We focused on the interactions of human Hsp70 with native Bw4 and its truncated and amino acid-substituted variants, because peptides bound to Hsp70 are postulated to have immunomodulatory effects such as T cell tolerance or activation in transplantation and tumor immunity. For example, it was reported that the 70-kDa heat shock proteins, Hsp70/Hsc70 bound to HLA-DRB1-derived peptide sequences comprising the shared epitope, such as HLA-DRB1*0401$^{65-77}$(KDLLEQKRAAVDT) and -DRB1*0101$^{65-77}$(KDLLEQRRAAVDT), which are considered to be associated with an increased risk for rheumatoid arthritis. This might be attributed to the enhanced activation of $CD4^+$ T cells against Hsp70/Hsc70-chaperoned antigen peptides via autophagy (15–17). Thus, the interaction between 70-kDa heat shock protein family and HLA molecules seems to provide some biological insights (18–21).

In searching for the peptide-binding motifs for the 70-kDa heat shock protein family, it was first reported that an endoplasmic reticulum protein, Bip, could bind to peptides containing at least seven residues with maximal affinity in the presence of ATPase activity (2, 3). It was also indicated that the peptide-

**TABLE 2**
**Binding assay of Ala-substituted peptides**

| Name | Sequence of alanine substitution | Binding affinity ($K_D$) |
|---|---|---|
| | | *M* |
| Bw4 | RENLRIALRY | $1.8 \times 10^{-6}$ |
| Bw4-R1A | AENLRIALRY | $1.1 \times 10^{-6}$ |
| Bw4-E2A | RANLRIALRY | $1.4 \times 10^{-6}$ |
| Bw4-N3A | REALRIALRY | $2.2 \times 10^{-6}$ |
| Bw4-L4A | RENARIALRY | $>10^{-3}$ |
| Bw4-R5A | RENLAIALRY | $>10^{-3}$ |
| Bw4-I6A | RENLRAALRY | $>10^{-3}$ |
| Bw4-L8A | RENLRIAARY | $>10^{-3}$ |
| Bw4-R9A | RENLRIALAY | $>10^{-3}$ |
| Bw4-Y10A | RENLRIALRA | $>10^{-3}$ |

| N3W | L4W | R5W | I6W | A7W | L8W | R9W | Y10W |
|---|---|---|---|---|---|---|---|
| N3Y | L4Y | R5Y | I6Y | A7Y | L8Y | R9Y | * |
| N3F | L4F | R5F | I6F | A7F | L8F | R9F | Y10F |
| N3R | L4R | * | I6R | A7R | L8R | * | Y10R |
| N3K | L4K | R5K | I6K | A7K | L8K | R9K | Y10K |
| N3H | L4H | R5H | I6H | A7H | L8H | R9H | Y10H |
| N3M | L4M | R5M | I6M | A7M | L8M | R9M | Y10M |
| N3I | L4I | R5I | * | A7I | L8I | R9I | Y10I |
| N3L | * | R5L | I6L | A7L | * | R9L | Y10L |
| N3V | L4V | R5V | I6V | A7V | L8V | R9V | Y10V |
| N3T | L4T | R5T | I6T | A7T | L8T | R9T | Y10V |
| N3A | L4A | R5A | I6A | * | L8A | R9A | Y10A |
| N3G | L4G | R5G | I6G | A7G | L8G | R9G | Y10G |
| N3P | L4P | R5P | I6P | A7P | L8P | R9P | Y10P |
| * | L4N | R5N | I6N | A7N | L8N | R9N | Y10N |
| N3S | L4S | R5S | I6S | A7S | L8S | R9S | Y10S |
| N3Q | L4Q | R5Q | I6Q | A7Q | L8Q | R9Q | Y10Q |
| N3D | L4D | R5D | I6D | A7D | L8D | R9D | Y10D |
| N3E | L4E | R5E | I6E | A7E | L8E | R9E | Y10E |

FIGURE 4. **Illustration of the Hsp70-peptide-binding motif.** An array of 126 single amino acid-substituted peptides was synthesized based on the Bw4 sequence (10-mer peptide). For example, in the case of substituted peptides at position 8 of the N terminus, Leu was substituted for by 18 different amino acid residues. These are represented as L8W, -Y, -F, -R, -K, -H, -M, -I, -V, -T, -A, -G, -P, -N, -S, -Q, -D, and -E in this figure. *White blocks* represent amino acids with preserved binding affinity for Hsp70 interaction ($K_D < 5 \times 10^{-6}$ M), whereas *blue blocks* indicate loss of binding affinity ($K_D > 1 \times 10^{-3}$ M). The *blocks* with *asterisks* indicate sequential peptides the same as the wild type.

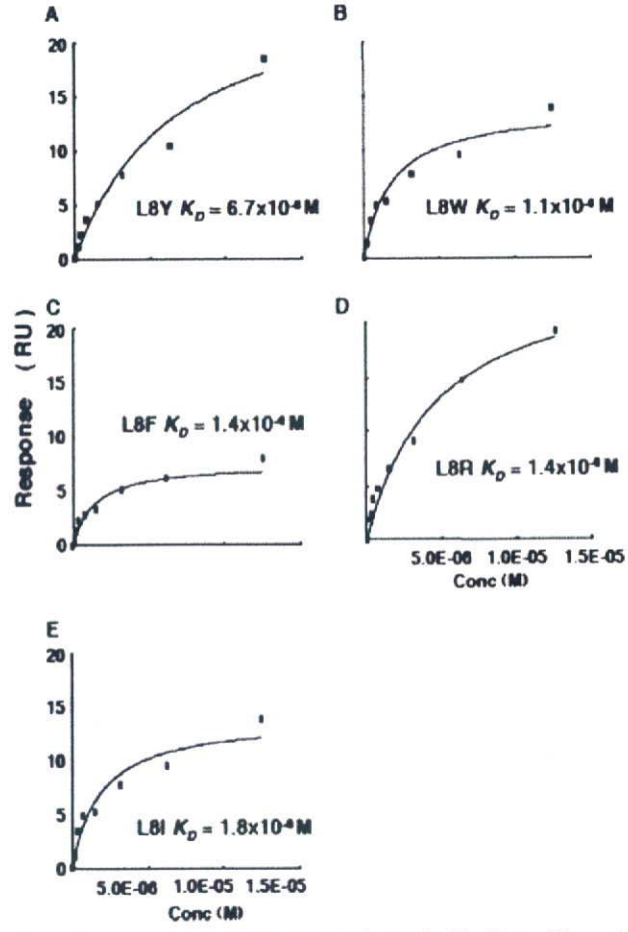


FIGURE 5. **A kinetic plot and binding isotherm for binding of five substituted peptides: L8Y (*A*), L8W (*B*), L8F (*C*), L8R (*D*), and L8I (*E*) to on Hsp70 sensor chip in concentrations ranging from 0.1 to 12.5 μM.** The $K_D$ value was determined using BIAevaluation version 4.1. *Conc*, concentration.

binding site of Bip showed a preference for sequences rich in aliphatic residues. Subsequently, from a study employing phage display library screening, the binding motif for Bip was revealed to be a heptapeptide with high contents of aromatic and hydrophobic residues (4). In the heptapeptide sequence, it was suggested that aromatic and hydrophobic residues occupied alternating positions. On the other hand, bacterial cytoplasmic 70-kDa heat shock protein homolog DnaK has a substrate-binding region in the C terminus, and repeated binding/release to substrates is dependent on the ATPase cycle at the ATPase domain of the N terminus (5, 6). Zhu *et al.* (7) reported the crystal structure of the C-terminal substrate-binding domain of DnaK, which was located in a hydrophobic substrate-binding cleft with a central pocket placed between a β sheet and two α helices. Basically, this domain is considered to bind to substrates by making hydrogen bonds (22). In addition, it was reported that a consensus motif recognized by DnaK consisted of peptides comprising a hydrophobic core of 4–5 residues flanked by basic residues (8). In the current study, the binding motif of the HLA-derived protein LRIALRY consisted of a hydrophobic core of 3 residues flanked by basic Arg residues.

Although such characteristics appeared to be similar to the consensus motif of DnaK, it was interesting that DnaK-Bw4 interaction was ~500-fold lower than Hsp70-Bw4 interaction. The substrate-binding domain of Hsp70 shares ~50% homology in its amino acid sequence with DnaK (18, 23). These structural differences might result in differences of binding affinity. For example, Fourie *et al.* (24) investigated the binding of 36

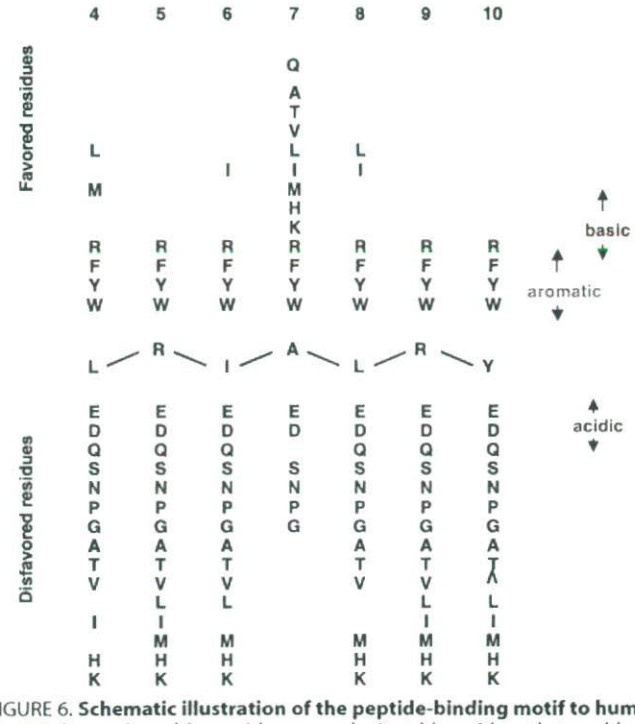


FIGURE 6. **Schematic illustration of the peptide-binding motif to human Hsp70.** Aromatic and Arg residues are substitutable residues that could preserve high affinity to Hsp70, suggesting that they are favored residues. In contrast, substitutions with acidic residues resulted in loss of binding affinity, suggesting that they are disfavored residues.

peptides to Hsc70, Bip, and DnaK by competition assay, demonstrating that there was little common peptide bound to these three proteins with similar binding affinity. It was also reported that mutant p53 protein-derived V10 peptide (substitution of Cys-126 by Tyr) was bound to Bip and DnaK but that V10-Hsc70 interaction was weaker than Bip and DnaK interaction (24). In our Biacore study, this appeared to be true, because the $K_D$ values for binding of Bip and DnaK to V10 peptide were estimated to be $4.28 \times 10^{-5}$ M and $2.26 \times 10^{-5}$ M, respectively. In contrast, that of Hsp70-V10 peptide was markedly lower ($K_D > 1 \times 10^{-3}$ M) than the Bip-and DnaK-V10 interaction (data not shown), which was consistent with their data (24). It is known that Hsp70/Hsc70 have very similar biochemical functions and are highly homologous proteins in their primary amino acid sequence except for a short heterologous C-terminal portion with an unknown biochemical function (18, 23, 25–27). Therefore, although we did not confirm the interaction between Hsc70 and V10 peptide, it is highly likely that this interaction could occur similarly to that of Hsp70 and V10 peptide in our current Biacore system.

In the peptide array experiments, when a residue in the LRIALRY motif was substituted for by an acidic residue, the binding affinity to Hsp70 was reduced in all cases. In the case of DnaK, acidic residues were excluded from cores and were found to be disfavored in the flanking region when 4360 peptides derived from 37 biologically relevant proteins were screened (8). In addition, Zhang and Oglesbee (13) reported similar results in which substitutions with acidic residues markedly reduced binding affinity to Hsp70. Thus, acidic residues appear to be disfavored in binding to the human 70-kDa heat shock protein family.

Meanwhile, it was reported that Hsp70 and Hsp90 could transfer peptides produced by the ubiquitin-proteasome system from the cytoplasmic milieu to the endoplasmic reticulum via transporters associated with antigen processing but not by natural diffusion (28, 29). These peptides were then bound to an endoplasmic reticulum-resident chaperone, GP96, and loaded onto major histocompatibility complex class I molecules in the endoplasmic reticulum (30–32). It was also reported that peptides bound to Hsp70 in tumor cells were identified as tumor antigens and that the purified tumor-derived Hsp70-peptide complex elicited tumor-specific cytotoxic T cell immunity *in vitro* and *in vivo* (33–36). We showed here that the new Hsp70-binding motif was a heptapeptide, LRIALRY. Interestingly, in this motif, aromatic residues or an Arg residue could be substituted at any position. These data might help elucidate the interaction of this motif with tumor antigens and suggest the possibility of construction of immunomodulatory cancer vaccines (35, 36).

Our study may also have several biologic implications. When we searched for homologous proteins with the Swiss-Prot data base, there were many such proteins with the same sequence in their primary amino acids as the LRIALRY motif. The majority of these proteins included HLA class I heavy chain molecules such as A*23, A*24, A*25, A*32, B*38, B*49, B*51, B*52, B*53, B*57, B*58, and B*59. When we extended the search for homologous sequences of proteins with residues favored in the motif as illustrated in Fig. 6, there were many human housekeeping proteins such as Hsp40 homologs, $\alpha$ adrenergic receptors, adenylate cyclase, protein ariadne-2, collagen $\alpha$-3 chain receptor, acetyl-CoA carboxylases, HLA class IIDQ4, DQ-DRW9, tyrosine-protein kinase JAK2, and many other proteins, and the number of such molecules was at least more than 317. In case of Hsp40 homologs among these 317 molecules, recent studies suggested that these protein-derived peptides efficiently activated $CD4^+CD25^+$ regulatory T cells (37–39). Therefore, one explanation for these data is that successful induction of immunosuppressive regulatory T cells might be attributable to Hsp40-derived peptides that could bind to Hsp70 with high affinity. Although the biologic significance of the current peptide-binding motif to Hsp70 is not yet clear, one immunological speculation is intriguing. There is a possibility that Hsp70-chaperoned peptides with our current motif may preferentially enter into the endoplasmic reticulum, make complexes with peptide-HLA class I, and subsequently be expressed on the cell surface. If these interactions happen in the thymus, our current observations might be compatible with the efficient induction of the negative selection of T cells, because peptides with this motif can be derived from not only self HLA class I heavy chains themselves but also many sets of self-housekeeping proteins.

*Acknowledgments—We thank Drs. Fumio Sugawara, Satoko Aoki, Mihoko Takami, Takeki Saito, and Yoichi Takakusaki of Science University of Tokyo for helpful assistance in this study.*

## REFERENCES

1. Bukau, B., and Horwich (1998) *Cell* **92**, 351–366
2. Flynn, G., Pohl, J., Flocco, M. T., and Rothman, J. E. (1991) *Nature* **353**, 726–730

3. Gething, M.-J., Blond-Elguindi, S., Buchner, J., Fourie, A., Knarr, G., Modrow, S., Nanu, L., Segal, M., and Sambrook, J. (1995) *Cold Spring Harbor Symp. Quant. Biol.* **60,** 417–428
4. Blond-Elguindi, S., Cwirla, S. E., Dower, W. J., Lipshutz, R. J., Sprang, S. R., Sambrook, J. F., and Gething, M. J. (1993) *Cell* **75,** 717–728
5. Szabo, A., Langer, T., Schröder, H., Flanagan, J., Bukau, B., and Hartl, F. (1994) *Proc. Natl. Acad. Sci. U. S. A.* **91,** 10345–10349
6. Buchberger, A., Schröder, H., Hesterkamp, T., Schönfeld, H.-J., and Bukau, B. (1996) *J. Mol. Biol.* **261,** 328–333
7. Zhu, X., Zhao, X., Burkholder, W. F., Gragerov, A., Ogata, C. M., Gottesman, M. E., and Hendrickson, W. A. (1996) *Science* **272,** 1606–1614
8. Rüdiger, S., Germeroth, L., Schneider-Mergener, J., and Bukau, B. (1997) *EMBO J.* **16,** 1501–1507
9. Hu, J., and Seeger, C. (1996) *Proc. Natl. Acad. Sci. U. S. A.* **93,** 1060–1064
10. Park, S. G., and Jung, G. (2001) *J. Virol.* **75,** 6962–6968
11. Zhang, X., Glendening, C., Linke, H., Parks, C. L., Brooks, C., Udem, S. A., and Oglesbee, M. (2002) *J. Virol.* **76,** 8737–8746
12. Zhang, X., Bourthis, J., Longhi, S., Carsillo, T., Buccellato, M., Morin, B., Canard, B., and Oglesbee, M. (2005) *Virology* **337,** 162–174
13. Zhang, X., and Oglesbee, M. (2003) *Biol. Proced. Online* **5,** 170–181
14. Nössner, E., Goldberg, J. E., Naftzger, C., Lyu, S. C., Clayberger, C., and Krensky, A. M. (1996) *J. Exp. Med.* **183,** 339–348
15. Gregersen, P., Silver, J., and Winchester, R. J. (1987) *Arthritis Rheum.* **30,** 1205–1213
16. Maier, J. T., Haug, M., Foll, J. L., Beck, H., Kalbacher, H., Rammensee, H. G., and Dannecker, G. E. (2002) *Immunogenetics* **54,** 67–73
17. Haug, H., Schepp, C. P., Kalbacher, H., Dannecker, G. E., and Holzer, U. (2007) *Eur. J. Immunol.* **37,** 1053–1063
18. Morimoto, R. I., Tissiéres, A., and Georgopoulos, C. (1994) *The Biology of Heat Shock Proteins and Molecular Chaperones*, pp. 111–284, Cold Spring Harbor Laboratory, Cold Spring Harbor, NY
19. Pockey, A. G. (2003) *Lancet* **362,** 469–476
20. Eden, W., Zee, R., and Prakken, B. (2005) *Nat. Rev. Immunol.* **5,** 318–330
21. Eisenlohr, L. C., Huang, L., and Golovina, T. N. (2007) *Nat. Rev. Immunol.* **7,** 403–410
22. Rüdiger, S., Schneider-Mergener, J., and Bukau, B. (2001) *EMBO J.* **20,** 1–9
23. Hunt, C., and Morimoto, R. I. (1985) *Proc. Natl. Acad. Sci. U. S. A.* **82,** 6455–6459
24. Fourie, A. M., Sambrooks, J. F., and Gething, M. J. (1994) *J. Biol. Chem.* **269,** 30470–30478
25. Dworniczak, B., and Mirault, M. E. (1987) *Nucleic Acids Res.* **15,** 5181–5197
26. Milner, C. M., and Campbell, R. D. (1990) *Immunogenetics* **32,** 242–251
27. MacAry, P. A., Javid, B., Floto, R. A., Smith, K. G. C., Oehlmann, W., Singh, M., and Lehner, P. J. (2004) *Immunity* **20,** 95–106
28. Li, Z., and Srivastava, P. K. (1994) *Behring Inst.* **94,** 37–47
29. Nieland, T. J. F., Tan, M. C. A., Monne-van Muijien, M., Koning, F., Kruisbeek, A. M., and Van Bleek, G. M. (1996) *Proc. Natl. Acad. Sci. U. S. A.* **93,** 6135–6139
30. Lammert, E., Arnold, D., Nijenhuis, M., Momburg, F., Hammerling, G. J., Brunner, J., Stevanovic, S., Rammensee, H. G., and Schild, H. (1997) *Eur. J. Immunol.* **27,** 923–927
31. Spee, P., and Neefjes, J. (1997) *Eur. J. Immunol.* **27,** 2441–2449
32. Srivastava, P. K., Udono, H., Blanchere, N., and Li, Z. (1994) *Immunogenetics* **39,** 93–98
33. Tamura, Y., Peng, P., Liu, K., Daou, M., and Srivastava, P. K. (1997) *Science* **278,** 117–120
34. Sato, K., Torimoto, Y., Tamura, Y., Shindo, M., Shinzaki, H., Hirai, K., and Kohgo, Y. (2001) *Blood* **98,** 1852–1857
35. Belli, F., Testori, A., Rivoltini, L. *et al.* (2002) *J. Clin. Oncol.* **20,** 4169–4180
36. Qian, J., Wang, S., Yang, J., Xie, J., Lin, P., Freeman, M. E., III, and Yi, Q. (2005) *Clin. Cancer Res.* **11,** 8808–8815
37. Prakken, B. J., Samodal, R., Le, T. D., Giannoni, F., Yung, G. P., Scavulli, J., Amox, D., Roord, S., Kleer, I., Bonnin, D., Lanza, P., Berry, C., Massa, M., Billetta, R., and Albani, S. (2004) *Proc. Natl. Acad. Sci. U. S. A.* **101,** 4228–4233
38. Nishikawa, H., Kato, T., Tawara, I., Saito, K., Ikeda, H., Kuribayashi, K., Allen, P. M., Schreiber, R. D., Sakaguchi, S., Old, L. J., and Shiku, H. (2005) *J. Exp. Med.* **201,** 681–686
39. Massa, M., Passalia, M., Manzoni, S. M., Campanelli, R., Ciardelli, L., Yung, G. P., Kamphuis, S., Pistorio, A., Meli, V., Sette, A., Prakken, B., Martini, A., and Albani, S. (2007) *Arthritis Rheum.* **56,** 1648–1657

# Expression of Livin in Renal Cell Carcinoma and Detection of Anti-livin Autoantibody in Patients

**Hiroshi Kitamura, Ichiya Honma, Toshihiko Torigoe, Hiroyuki Hariu, Hiroko Asanuma, Yoshihiko Hirohashi, Eiji Sato, Noriyuki Sato, and Taiji Tsukamoto**

**OBJECTIVES** To assess the expression of livin, a member of the inhibitor of apoptosis protein family, in renal cell carcinoma (RCC) and to determine its prognostic relevance.

**METHODS** Immunohistochemical staining for livin was performed using paraffin-embedded tissues from 45 cases of RCC. Then we assessed anti-livin antibodies (Abs) in patient sera by enzyme-linked immunosorbent assay and Western blotting. Disease-specific survival of patients was assessed, and differences between the immunohistologically livin-positive and livin-negative groups and between the anti-livin Ab-positive and anti-livin Ab-negative groups were compared with recurrence-free survival using the Kaplan-Meier method and log-rank test.

**RESULTS** Of the 45 RCC specimens, 26 (57.8%) showed positive staining of livin immunohistochemically. In the RCC patients, anti-livin antibodies were detected and their levels were significantly higher than those in healthy volunteers. However, there was no difference in disease-specific survival between the livin-positive and livin-negative patients or between the anti-livin-positive and anti-livin-negative patients.

**CONCLUSIONS** Although livin expression may not provide predictive information, it may be recognized as a tumor antigen by the immune system in RCC patients. UROLOGY 70: 38–42, 2007. © 2007 Elsevier Inc.

Livin is a member of the inhibitor of apoptosis protein (IAP) family.[1] It is a protein with a single baculoviral IAP repeat domain and a COOH-terminal RING domain, and it can inhibit apoptosis by inhibiting proteolytic activation of caspases 3, 7, and 9.[2] Livin is not present in most normal adult differentiated tissues, although its messenger ribonucleic acid and the protein are present in the fetal brain, kidney, and placenta.[1,3] It is expressed in malignant melanoma cells, and it could be one of the immunodominant tumor antigens in melanoma patients.[4] It is also expressed in lung cancer,[5] colon cancer, prostate cancer, B cell lymphoma, erythroleukemia, and promyelocytic leukemia cell lines.[6] The antiapoptotic activity of livin is more robust than that of survivin,[1] another member of the IAP family that has been demonstrated in colorectal cancer, non-small-cell lung cancer, gastric cancer, bladder cancer, breast cancer, melanoma, neuroblastoma, hepatocellular carcinoma, diffuse large B cell lymphoma,[7] and renal cell carcinoma (RCC).[8] Though there have been a number of reports[1,5,6] demonstrating its expression in various malignancies, livin expression in RCC and its antigenic potential have not yet been elucidated.[8]

Herein we assess the expression of livin in RCC cells and tissues and study the correlation between its expression and prognosis. Serologic responses against livin were also examined in RCC patients and healthy volunteers. Our study highlights livin as a novel tumor-specific antigen in RCC.

## MATERIAL AND METHODS

### Immunohistochemical Staining for Livin

We reviewed the clinical pathology archives of 138 consecutive patients who underwent radical or partial nephrectomy and were diagnosed as having clear cell RCC at the Sapporo Medical University Hospital, Sapporo, Japan from May 1991 to August 1998. Patients whose medical records were incomplete or who had a history of another cancer were excluded. We selected 45 patients on the basis of the availability of sufficient material for immunohistochemistry and enzyme-linked immunosorbent assay (ELISA). The median age at operation for the 27 male and 18 female patients was 61 years (range, 24 to 80). All hematoxylin and eosin-stained slides were reviewed, and clinical stage was assigned according to the 2002 TNM classification of malignant tumors. All of these specimens were histopathologically diagnosed as clear cell carcinoma. There

*This study was supported in part by the Stiftelsen Japanese-Swedish Cooperative Foundation and by Grants-in-Aid from the Japan Society for the Promotion of Science (17390441).*

*From the Departments of Urology and Pathology, Sapporo Medical University School of Medicine, Sapporo, Japan*

*Reprint requests: Hiroshi Kitamura, M.D., Ph.D., Department of Urology, Sapporo Medical University School of Medicine, South 1 West 16, Chuo-ku, Sapporo 060-8543, Japan. E-mail: hkitamu@sapmed.ac.jp*

*Submitted: October 6, 2006; accepted (with revisions): March 13, 2007*





0090-4295/07/$32.00
doi:10.1016/j.urology.2007.03.040

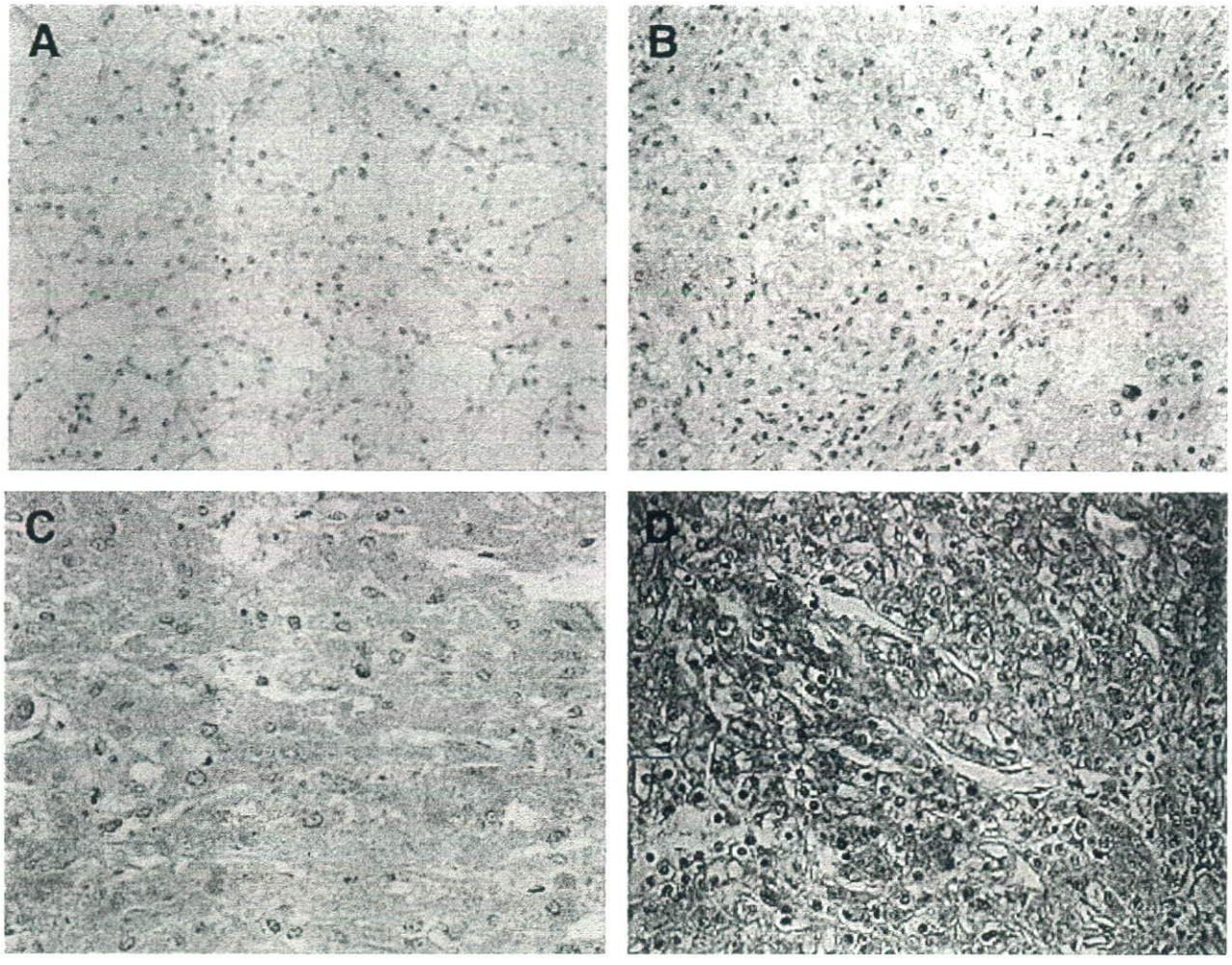


**Figure 1.** Representative pictures of immunohistochemical staining with a monoclonal antibody reacting to livin in RCC. **(A)** Score 0; **(B)** score 1; **(C)** score 2; **(D)** score 3.

were 22 cases of clinical Stage 1, 9 cases of Stage 2, 7 cases of Stage 3, and 7 cases of Stage 4. The Fuhrman grade distribution was 15 cases with grade 1 to 2, 22 cases with grade 3, and 8 cases with grade 4. Median tumor diameter was 5.5 cm (range, 1.2 to 18 cm). All patients were followed up every 3 months during the first 3 years after surgery, every 6 months from 3 to 10 years, and annually after 10 years. The median follow-up period was 63 months (range, 3 to 117 months). All patients with Stage 3 and 4 disease underwent cytokine-based immunotherapies after surgery. Six (19.4%) of the 31 Stage 1 and 2 patients underwent such therapies when a recurrent tumor was detected during follow-up.

Immunohistochemical staining with a monoclonal anti-livin antibody established in our laboratory was performed on 5-$\mu$m-thick, formalin-fixed, paraffin-embedded tissue sections by the method previously described.[5] All specimens were reviewed independently using light microscopy by investigators who were blinded to clinicopathologic data (H.K., I.H., and T.T.). For the staining of livin, the mean percentage of positive tumor cells was determined in at least five areas at ×400 magnification. The cells that expressed livin were classified qualitatively into four categories (0, 1+, 2+, and 3+) according to the intensity of staining and the percentage of cells: 0, less than 10% of cancer cells with positive staining; 1+, low to moderate staining in 11% to 30% of cells; 2+, moderate to strong staining in 31% to 50% of cells; and 3+, diffuse strong staining in more than 50% of cells (Fig. 1).[9] If a specimen showed a staining pattern that did not fit into one of the categories, the pathologists scored it according to their judgment. The specimens were classified as normal (category 0) or as abnormal (categories 1 to 3). Any immunoreactivity was considered positive because livin is undetectable in normal adult tissue.[5]

### ELISA for Anti-livin Antibody in Patient Sera

Blood samples were collected from the 45 RCC patients who underwent the immunohistochemical analysis described above before surgery and from 21 healthy volunteers (age range, 22 to 65 years) after receipt of informed consent. After centrifugation, sera were divided into aliquots and stored at −80°C. ELISA was performed as previously described.[10] Data were obtained in triplicate for each sample.

### Western Blot Analysis of Serum Anti-livin Antibody

The livin complementary deoxyribonucleic acid (cDNA) fused with the myc tag was cloned into BamHI and EcoRI sites of pcDNA3.1 mammalian expression vector (Invitrogen, Carlsbad, Calif). 293T human embryonal kidney cells were transfected with the plasmid by using Lipofectamine 2000 (Invitrogen). Forty-eight hours after the transfection, cell lysates were prepared from livin-transfected cells and wild-type 293T cells,

**Table 1.** Relationship between livin expression and clinicopathologic factors of patients with renal cell carcinoma

| Factors | Total (n = 45) | Livin Expression | | P Value |
|---|---|---|---|---|
| | | Negative (n = 19) | Positive (n = 26) | |
| Clinical stage | | | | 0.344 |
| 1 | 25 | 13 (52.0) | 12 (48.0) | |
| 2 | 6 | 1 (16.7) | 5 (83.3) | |
| 3 | 7 | 2 (28.6) | 5 (71.4) | |
| 4 | 7 | 3 (42.9) | 4 (57.1) | |
| Fuhrman grade | | | | 0.093 |
| 1/2 | 8 | 6 (75.0) | 2 (25.0) | |
| 3 | 26 | 10 (38.5) | 16 (61.5) | |
| 4 | 11 | 3 (27.3) | 8 (72.7) | |
| Tumor diameter (cm) | | | | 0.460 |
| ≤7 | 28 | 21 (75.0) | 7 (25.0) | |
| >7 | 17 | 11 (64.7) | 6 (35.3) | |
| Tumor necrosis | | | | 0.060 |
| No | 33 | 26 (78.8) | 7 (21.2) | |
| Yes | 12 | 6 (50.0) | 6 (50.0) | |
| Perirenal fat invasion | | | | 0.744 |
| No | 42 | 18 (42.9) | 24 (57.1) | |
| Yes | 3 | 1 (33.3) | 2 (66.7) | |
| Tumor thrombus | | | | 0.418 |
| No | 38 | 17 (44.7) | 21 (55.3) | |
| Yes | 7 | 2 (28.6) | 5 (71.4) | |
| Distant metastasis | | | | 0.971 |
| No | 38 | 16 (42.1) | 22 (57.9) | |
| Yes | 7 | 3 (42.9) | 4 (57.1) | |
| Anti-livin antibody | | | | 0.005 |
| Negative | 20 | 13 (65.0) | 7 (35.0) | |
| Positive | 25 | 6 (24.0) | 19 (76.0) | |

Values in parentheses are percentages.

respectively, in 1 mL of radioimmunoprecipitation assay (RIPA) buffer supplemented with a protease inhibitor mixture tablet (Roche Molecular Biochemicals, Indianapolis, Ind). Then the lysates were used for immunoprecipitation with an anti-myc monoclonal antibody conjugated to agarose (Santa Cruz Biotechnology, Santa Cruz, Calif). The samples were washed three times with RIPA buffer, boiled in Laemmli buffer, and resolved by sodium dodecylsulfate polyacrylamide gel electrophoresis. The proteins were transferred to polyvinylidene diflouride membranes (Immobilon-P, Milipore, Bedford, Mass), which were then incubated with serum samples diluted 1:10 or an anti-livin polyclonal antibody (1.0 mg/L, original) followed by a 1:2000 dilution of rabbit antihuman immunoglobulin G (IgG) F(ab')2 or goat antirabbit IgG F(ab')2 conjugated with horseradish peroxidase (DakoCytomation, Glostrup, Denmark). The immunocomplex was visualized by enhanced chemiluminescence according to the manufacturer's specifications (Amersham Biosciences, Piscataway, NJ).

### Statistical Analysis

The chi-square test was used for comparison of data among groups. We compared the values for the anti-livin antibody between the two groups by using the Wilcoxon test. Disease-specific survival was assessed by the Kaplan-Meier method, and differences between the two groups were compared using the log-rank test. Univariate and multivariate regression analyses according to the Cox proportional hazards regression model, with disease-specific survival as the dependent variable, were used to evaluate livin expression and anti-livin antibody as potential independent prognostic factors. $P < 0.05$ was considered to indicate statistical significance. The calculations were performed with JMP software (SAS Institute, Cary, NC).

## RESULTS

### Expression of Livin in RCC Tissues

By immunohistochemical staining, livin was detected in 26 (57.8%) of the 45 RCC specimens. There were 19 cases of staining score 0, 15 cases of score 1, 3 cases of score 2, and 8 cases of score 3. The association between livin expression and clinicopathologic characteristics is shown in Table 1.

### Serum Anti-livin Antibody in RCC Patients

The absorbance value of ELISA detecting the anti-livin antibody in sera from RCC patients and healthy volunteers was 0.17 ± 0.09 and 0.08 ± 0.03, respectively (Fig. 2A). The cutoff value for the positivity in the anti-livin ELISA was determined from the absorbance values of healthy volunteers' samples as the mean absorbance value + 2 standard deviations (SD) (0.14). On the basis of this criterion, serum samples from 25 (55.6%) of the 45 patients were positive for the anti-livin autoantibody. However, there was no significant relationship between anti-livin autoantibody and any clinicopathologic factor.

Western blot analysis for the serum anti-livin antibody in an RCC patient demonstrated immunoreactivity to

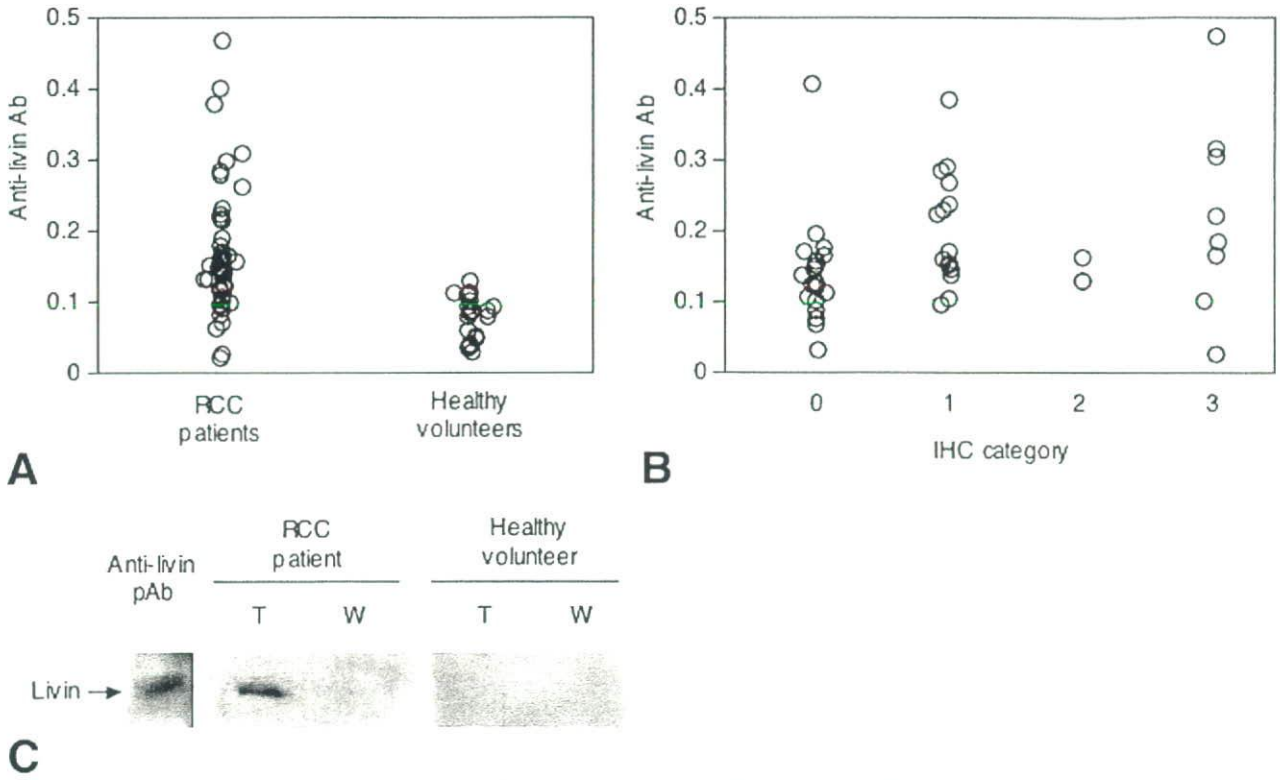


**Figure 2. (A)** Serum anti-livin antibodies of healthy volunteers and RCC patients. **(B)** Serum anti-livin antibody titers and categories of immunohistochemistry (IHC) in RCC tissues. **(C)** Western blot analysis for immunoreactivity of serum to livin protein in 293T cell lysates. Lane 1, positive control of polyclonal anti-livin antibody. Lanes 2 and 3, serum from an RCC patient. Lanes 4 and 5, serum from a healthy volunteer. pAb = polyclonal antibody; T = livin-transfected 293T cell lysate; W = wild-type 293T cell lysate.

livin protein expressed in the livin cDNA-transfected 293T cells. There was no immunoreactivity in serum from a healthy volunteer (Fig. 2B).

The mean (± SD) absorbance value of the anti-livin antibody in patients with livin-positive RCC and in patients with livin-negative RCC was 0.20 ± 0.10 and 0.13 ± 0.08, respectively. There was a significant difference in the values between the two groups ($P = 0.013$).

### Association of Livin Expression or Anti-livin Antibody with Disease-Specific Survival

The 5-year disease-specific survival was 81.6% for all patients. Univariate analysis revealed that pathologic T stage, TNM stage, and tumor diameter were significant factors influencing disease-specific survival of patients with RCC (Table 2). Multivariate analysis revealed no significant factor that affected disease-specific survival. In both analyses neither livin expression nor the anti-livin antibody was a significant factor. The 5-year survival rate was 81.7% and 81.2% in the livin-positive and livin-negative arms, respectively (Fig. 3A). The 5-year survival rate was 81.1% and 82.3% in the anti-livin Ab-positive and anti-livin Ab-negative arms, respectively (Fig. 3B). There was no difference between the two groups in either comparison. Moreover, there was no difference in survival among the four groups stratified according to immunohistochemistry scores.

**Table 2. Results of univariate Cox regression analysis for disease-specific survival**

| Factors | Risk Ratio Label (95% Confidence Interval) | *P* Value |
|---|---|---|
| Clinical stage | 1.78 (1.05–3.11) | 0.033 |
| Fuhrman grade | 2.07 (0.78–6.12) | 0.147 |
| Tumor diameter | 3.99 (1.05–18.0) | 0.042 |
| Pathologic T stage | 1.70 (1.08–2.72) | 0.022 |
| Tumor necrosis | 0.79 (0.12–3.27) | 0.762 |
| Livin expression | 1.91 (0.47–7.25) | 0.347 |
| Anti-livin antibody | 1.02 (0.27–4.13) | 0.975 |

## COMMENT

To the best of our knowledge this is the first report demonstrating livin expression in RCC. Fifty-eight percent of the RCC cases expressed livin immunohistochemically, but there was no relationship between livin expression in tumors and any clinicopathologic parameter or disease-specific survival. In other words, livin may not be a prognostic marker for RCC. In contrast, Parker *et al.*[11] have reported that expression of survivin, another IAP family member, is an independent predictor of clear cell RCC progression. Although there are limitations due to the small sample size and the relatively better prognosis in this study, our results suggest that the characteristics and role of livin in RCC progression might be different from those of survivin.